ELSEVIER

Nuclear Physics A 621 (1997) 719–735

NUCLEAR PHYSICS A

Study of the Gamow–Teller resonance in ^{90}Nb and ^{208}Bi

Nguyen Dinh Dang [a,1], Akito Arima [a], Toshio Suzuki [b], Shuhei Yamaji [a]

[a] *Cyclotron Laboratory, RIKEN, 2-1 Hirosawa, Wako, Saitama 351-01, Japan*

[b] *Department of Physics, College of Humanities and Sciences, Nihon University, Sakurajosui 3-25-40, Setagaya-ku, Tokyo 156, Japan*

Received 18 April 1997; revised 25 November 1997

Abstract

An approach is proposed for studying the spreading properties of the Gamow–Teller resonance (GTR) in heavy nuclei including the coupling to $2p2h$ configurations and the ground-state correlations beyond RPA. The GTR is generated by a proton p–neutron h (πp–νh) phonon within the renormalized RPA. The second-order configuration mixing beyond RPA is realized by constructing two-phonon configurations, in which one of two intermediate phonon states is a πp–νh phonon. The numerical calculations are performed in the parent nuclei ^{90}Zr and ^{208}Pb making use of M3Y nucleon–nucleon interaction and the single-particle wave functions obtained in the standard harmonic oscillator potential. The single-particle energies around the Fermi surface are substituted with the empirical values or those given by a Woods–Saxon potential. The results obtained provide a reasonable account for recent experimental findings on the GTR in these nuclei. The extension of the present approach to highly excited (hot) nuclei is also provided. The GTR is found to be stable against temperatures up to $T \approx 6$ MeV. © 1997 Elsevier Science B.V.

PACS: 24.30.Cz; 21.10.Pc; 21.60.-n; 25.40.Kv

Keywords: Giant resonance; Spreading width; Quenching of Gamow–Teller resonance; Random-phase approximation; $2p2h$ configuration mixing; (p,n) reaction

1. Introduction

The giant Gamow–Teller resonance (GTR) has been one of the interesting subjects of both experimental and theoretical investigations for more than thirty years. This

[1] Research fellow of the Science and Technology Agency of Japan.

PII S0375-9474(97)00172-3

collective spin–isospin excitation was predicted in 1963 [1] to explain the hindrance of allowed unfavored β decays. Its first experimental observation has been reported in 1975 in the ^{90}Zr(p,n) reaction [2], which has been a powerful tool in the study of the GTR in heavy nuclei at intermediate energies.

A measure of the total observed transition strength for the GTR is provided by the model-independent Ikeda sum rule [1]: $S_{\beta_-} - S_{\beta_+} = 3(N-Z)$. As the inverse β-decay $\sigma\tau_+$ is strongly hindered because of the Pauli principle, $3(N-Z)$ should be nearly exhausted by the transition strength summed over all GT states in the daughter $(Z+1, N-1)$ nucleus. However, until very recently (see below) experimental systematics over a wide range of the periodic table found only around 60% of the sum rule value on the average. This so-called *quenching* of the GTR is still an unresolved problem requiring further efforts in both theoretical and experimental studies.

Already in the early 1970s Wilkinson [3] urged nuclear physicists to look at the super-allowed β-decay rates of light nuclei with a valence nucleon or hole outside an LS doubly closed shell. It turns out that some of them, such as ^{39}Ca $\rightarrow$ ^{39}K and ^{41}Sc $\rightarrow$ ^{41}Ca, have been observed to be very much hindered down to 66% or 74% of their single-particle values [4]. If they are squared, they amount only to 44% or 54% of their single-particle transition probabilities. In order to explain these quenchings, the importance of $2p1h$ configuration mixing has been pointed out [5]. However, after the quenching of the GTR was confirmed, another mechanism was proposed. This is the $\Delta(1232)$ isobar–hole admixtures in the nuclear wave function [6]. Theoretical studies have shown that this effect seems to be small in light and medium nuclei [7,8] or can be only of the order of 10~20% in heavy nuclei [9]. Instead of $2p1h$ admixtures the $2p2h$-configuration mixing must be taken into account. If this mechanism plays an important role, the missing GT strength should be spread over the physical background below and beyond the GTR [9,10].

The first perturbative calculation of the mixing of GT strength with $2p2h$ configurations at high excitation energies in ^{90}Zr has been performed by Bertsch and Hamamoto [11] who found that roughly 50% of the GT strength is shifted into the region of 10–45 MeV. The M3Y interaction including a tensor part was used in this calculation. Since the tensor force is of the longest range in the momentum space it may couple the $1p1h$ states to very high-lying $2p2h$ states, causing a more fragmentation of the strength toward higher excitation energies. The authors of Ref. [8] found that the effects of mixing of highly excited configurations through a tensor force is essential to explain the large reduction of the GT-type β-decay matrix element in light nuclei. For medium and heavy nuclei this has been confirmed by the calculations in ^{40}Ca, ^{90}Zr, and ^{208}Pb by Drożdż et al. [12] within the projected second RPA (SRPA). These calculations used a two-body interaction derived from a G-matrix with the HM3A version of the Bonn potential. The results show that the GTR in these nuclei has a long tail, which extends up to excitation energies of more than 50 MeV. Recently Udagawa et al. applied a continuum TDA approach including an empirical width of GTR via the imaginary part of the optical potential [13]. The results of their calculations in ^{208}Pb turned out to be close to those of Drożdż et al. [12].

Meanwhile the fragmentation of the GTR in heavy nuclei has also been calculated by Kuzmin and Soloviev [14] within the framework of the quasiparticle-phonon model (QPM) [15]. In the QPM one first solves the RPA to determine the collective *ph* (phonon) excitations. The $2p2h$ configuration mixing is realized via coupling to two-phonon states. This two-step procedure, which reduces largely the dimension of matrices under consideration, is one of advantages of this approach as compared to the SRPA [12]. The results of the calculations within the QPM, using the single-particle energies from the Woods–Saxon potential and the separable force as residual interaction, showed, however, that the GTR spreads only up to the excitation energies of around 30 MeV.

Colò et al. calculated spreading of GTR within the framework of a continuum TDA + Hartree–Fock formalism with several types of Skyrme interaction [16]. In their calculations the $1p1h$–$2p2h$ configuration mixing was simulated by coupling TDA states to low-lying collective vibration modes. The calculated energy for the main peak of the GTR is higher than the experimental value by about 2∼4 MeV depending on the version of Skyrme interaction. The strength distribution was shown only in the localization of GTR within the interval around (18∼24) MeV, where the strength amounts to 61∼68% of the Ikeda sum rule. Both strength functions in Refs. [14,16] correspond to a width of GTR smaller by 18∼20% as compared to the experimental value. In addition the results in Ref. [16] were found to be quite sensitive to the type of Skyrme interaction in use. Even though all theoretical models recover the Ikeda sum rule in the energy interval below 50∼60 MeV, the amount of strength in the GTR region as well as the shape of the strength function itself vary noticeably depending on models.

Recently high-resolution measurements for the proton decay from GTR in the ^{208}Pb(^{3}He,t)^{208}Bi reaction at $E(^{3}\mathrm{He}) = 450$ MeV [17] and for the differential cross-sections for the ^{90}Zr$(p,n)^{90}$Nb reaction at 295 MeV [18] were carried out at the Research Center for Nuclear Physics (RCNP) in Osaka. In particular, the authors of Ref. [18] were able to extract, for the first time, the $L = 0$ cross section in the continuum. It results in a long tail of GTR extending up to around 60 MeV, recovering the missing part of the GTR strength. These data also show clearly that the contribution from isobar–hole admixtures is less than 6% of the GTR sum rule.

These new experimental results [17,18] have motivated the present work. We are going to try here an approach to the damping of GTR based on the coupling of the GTR excitations in the RPA to $2p2h$ configurations via two-phonon states. Even though the way of constructing the $2p2h$ configuration mixing is similar to the one within the QPM [15], the essential difference is in the use of a two-body residual interaction in the form of the M3Y effective nucleon–nucleon force in our approach instead of a separable one. Another improvement is that the effects of ground-state correlations beyond RPA and of the two-phonon backward processes are also included in our calculations. In contrast to the approach in Ref. [16], we shall couple πp–νh configurations also to high-lying $2p2h$ (two-phonon) states. Finally our formalism allows us to extend the numerical calculations to non-zero temperature case.

The formalism of our approach is discussed in Section 2. The RPA-like equation for *ph* (phonon) excitations including the ground-state correlations beyond the usual

RPA is outlined in Section 2.1. The formalism for calculating the spreading of the GTR strength function after coupling πp–νh phonon states to two-phonon ones is presented in Section 2.2. The details and results of numerical calculations for the GTR in ^{90}Nb and ^{208}Bi are discussed in Section 3, where the comparison to the recent experimental data and the data given by the models in Refs. [12–14,16] is made. The paper is summarized in the last section.

2. Formalism

2.1. Ground-state correlations beyond RPA

The usual RPA violates the Pauli principle by treating ph creation $B^\dagger_{ph}$ and annihilation B_{ph} operators as ideal bosons. As a consequence RPA breaks down at a certain value of the interaction strength, where it yields imaginary values. A simple approach to correct for this deficiency has been proposed by Hara [19]. This induced the ground-state correlations beyond the RPA, which can be taken into account by solving a non-linear RPA-like equation. Recently an improvement of this method has been proposed in Ref. [21], where a higher accuracy in expansion series was achieved and realistic self-consistent calculations with Skyrme interaction were performed for the first time for lowest quadrupole and octupole states in heavy nuclei. In the present paper we would like to include this effect in the calculations of the GTR. As the detail of this method has been already discussed in Ref. [21], we outline it here only in brief.

The pp and hh pair operators can be expressed in terms of ph pair ones ($B^\dagger_{ph} \equiv a^\dagger_p a_h$) using the mapping procedure as in Ref. [20]:

$$B^\dagger_{pp'} \to \sum_h B^\dagger_{ph} B_{p'h}, \qquad B^\dagger_{hh'} \to \delta_{hh'} - \sum_p B^\dagger_{ph'} B_{ph}. \tag{2.1}$$

The many-body Hamiltonian is then approximated in terms of only ph pair operators $B^\dagger_{ph}$ and B_{ph} as

$$H = H_0 + H_V, \tag{2.2}$$

where H_0 is diagonalized in RPA, while H_V is responsible for the configuration mixing beyond RPA. The *renormalized* phonon operator, generating the collective ph excitation is introduced in RPA as:

$$Q^\dagger_\nu = \sum_{ph} D^{-1/2}_{ph} [X^\nu_{ph} B^\dagger_{ph} - Y^\nu_{ph} B_{ph}]. \tag{2.3}$$

The presence of the renormalization factor $(D_{ph})^{-1/2}$ $(n_h > n_p)$ in Eq. (2.3) preserves the boson nature of $Q^\dagger_\nu$ and Q_ν within the approximation

$$\langle 0|[B_{ph}, B^\dagger_{p'h'}]|0\rangle = \langle 0|B^\dagger_{hh}|0\rangle - \langle 0|B^\dagger_{pp}|0\rangle \equiv \delta_{pp'}\delta_{hh'} D_{ph}, \tag{2.4}$$

in such a way that the amplitudes X^ν_{ph} and Y^ν_{ph} still satisfy the RPA normalization and closure relations. The factor D_{ph} characterizes the correlations beyond those, which are

already included in the RPA ground state $|0\rangle$. These ground-state correlations beyond RPA restore (up to second order in *ph* operators) the Pauli principle, which is violated when using $B^{\dagger}_{ph}$ and B_{ph} as ideal bosons. The expression for D_{ph} has been derived in Ref. [21] more generally than the one in Ref. [19]. It can be extended further here to non-zero temperature T by replacing the average over the ground state $\langle 0|\ldots|0\rangle$ (at $T=0$) with the one over the thermal equilibrium ensemble ($T \neq 0$):

$$\langle|\ldots|\rangle = \frac{\mathrm{Tr}[\ldots \exp^{-H_0/T}]}{\mathrm{Tr}\exp^{-H_0/T}}. \tag{2.5}$$

The final expression has the form

$$D_{ph} = 1 - \sum_{p'\nu} D_{p'h}[(1+N_\nu)(Y^{\nu}_{p'h})^2 + N_\nu (X^{\nu}_{p'h})^2] - \sum_{h'\nu} D_{ph'}[(1+N_\nu)(Y^{\nu}_{ph'})^2 + N_\nu (X^{\nu}_{ph'})^2]. \tag{2.6}$$

The *phonon number* N_ν in Eq. (2.6) arises from the approximation

$$\langle|Q^{\dagger}_{\nu}Q_{\nu'}|\rangle \approx \delta_{\nu\nu'}\langle|Q^{\dagger}_{\nu}Q_{\nu}|\rangle \equiv \delta_{\nu\nu'}N_\nu. \tag{2.7}$$

Eqs. (2.6) and (2.7) can be used to unify the quantal correlations in the ground state and the thermal fluctuations at non-zero temperature if we describe the phonon number N_ν by the Bose–Einstein statistics at $T \neq 0$ as

$$N_\nu = (e^{\omega_\nu/T} - 1)^{-1}, \tag{2.8}$$

with ω_ν being the energy of one-phonon excitation. At $T=0$ the phonon number N_ν vanishes and one recovers the equation for D_{ph} in Ref. [21]. The case with $D_{ph}=1$ means no ground-state correlations beyond RPA.

The *RPA-like equation* (renormalized by the factor D_{ph}) has the same form as the conventional one with the two-body interaction multiplied by $(D_{ph}D_{p'h'})^{1/2}$ (see Refs. [19,21]). Because of Eq. (2.6) it becomes a non-linear equation with respect to the amplitude Y and must be solved self-consistently together with Eq. (2.6). Its solution defines the energy ω_ν and the amplitudes X and Y of the *ph* excitation generated by the phonon operator in Eq. (2.3).

Specifying in Eq. (2.3) the p_π indices denoting proton particles and h_ν – neutron holes, we can define the charge-exchange πp–νh phonon (creation) operator $\mathcal{Q}^{\dagger}_{\alpha}$ as

$$\mathcal{Q}^{\dagger}_{\mu} = \sum_{p_\pi h_\nu} D^{-1/2}_{p_\pi h_\nu}[X^{\mu}_{p_\pi h_\nu}B^{\dagger}_{p_\pi h_\nu} - Y^{\mu}_{p_\pi h_\nu}B_{p_\pi h_\nu}]. \tag{2.9}$$

The GT excitations are generated by acting operator $\mathcal{Q}^{\dagger}_{\mu}$ on the ground state $|0\rangle$ of the even–even parent nucleus. The renormalized RPA-like equation for the charge-exchange excitations, generated by phonon operator πp–νh $\mathcal{Q}^{\dagger}_{\alpha}$ in Eq. (2.9), has the same form as the one for *ph* phonon excitations. Therefore we omit writing down it here.

2.2. Spreading of GTR due to mixing with two-phonon configurations

The coupling of the charge-exchange πp–νh phonon excitations, generated by operator $\mathcal{Q}^\dagger$ in Eq. (2.9), to the ones caused by phonon $\{Q^\dagger, Q\}$ operators in Eq. (2.3), is the second-order configuration mixing, which leads to the spreading (fragmentation) of the GTR in RPA. Our study later on will concern only the average quantities such as strength function, the energies, spreading properties. Hence we will work with the expectation values $\langle 0|\ldots|0\rangle$ (at $T = 0$) or $\langle|\ldots|\rangle$ ($T \neq 0$) rather than with wave functions. This makes straightforward the extension of our formalism to non-zero temperature, where a pure ground state cannot be defined. In this general case the two-time Green function method [22,23] turns out to be a powerful tool in studying the damping of collective motion. This method has been applied within the QPM in calculating the $E\lambda$ (natural parity) transitions including giant resonances at zero as well as non-zero temperature [24]. The fragmentation of GTR in the present paper can be studied considering the following two-time Green functions, which describe

(1) the propagation of the ph phonon:

$$G^{-,+}_{\alpha;\alpha'}(t-t') = \langle\langle \mathcal{Q}_\alpha(t); \mathcal{Q}^\dagger_{\alpha'}(t')\rangle\rangle, \tag{2.10}$$

(2) the propagation of charge-exchange πp–νh phonon:

$$\mathcal{G}^{-,+}_{\alpha;\alpha'}(t-t') = \langle\langle \mathcal{Q}_\alpha(t); \mathcal{Q}^\dagger_{\alpha'}(t')\rangle\rangle, \tag{2.11}$$

(3) the mixing with two-phonon configurations:

$$\mathcal{G}^{--,+}_{\beta\gamma;\alpha'}(t-t') = \langle\langle \mathcal{Q}_\beta(t)\mathcal{Q}_\gamma(t); \mathcal{Q}^\dagger_{\alpha'}(t')\rangle\rangle, \tag{2.12}$$

and their backward processes described by $\mathcal{G}^{+,+}_{\alpha;\alpha'}(t-t') \equiv \langle\langle \mathcal{Q}^\dagger(t); \mathcal{Q}^\dagger(t')\rangle\rangle$ and $\mathcal{G}^{++,+}_{\beta\gamma;\alpha'}(t-t') \equiv \langle\langle \mathcal{Q}^\dagger_\gamma(t)\mathcal{Q}^\dagger_\beta(t); \mathcal{Q}^\dagger_{\alpha'}(t')\rangle\rangle$. In Eqs. (2.10)–(2.12) the standard notation for the two-time Green function from Refs. [22,23] is used. We notice that in the $2p2h$ configuration mixing described by Green function $\mathcal{G}^{--,+}_{\beta\gamma;\alpha'}(t-t')$ in Eq. (2.12), the two-phonon configuration is constructed by one charge-exchange phonon $\mathcal{Q}^\dagger$ and one *ph* phonon $Q^\dagger$. The physical processes included in our approach can be depicted diagrammatically in Fig. 1.

The set of equations for the Green functions in Eqs. (2.10)–(2.12) and their backward processes is derived following the standard procedure in Ref. [23]. As the structure of *ph* and charge-exchange phonons is known after solving the renormalized RPA-like equations in the previous section, the Hamiltonian in Eq. (2.2) can be expressed in terms of phonon operators $\{Q^\dagger, Q\}$ and $\{\mathcal{Q}^\dagger, \mathcal{Q}\}$. This makes the procedure of deriving the equation for Green functions straightforward. It results in a hierarchy of equations including higher-order Green functions as well. In order to close the set up to the functions defined above we use Eq. (2.7) to decouple, e.g.

$$\langle\langle Q^\dagger_\mu \mathcal{Q}_{\mu'}\mathcal{Q}_\nu; \mathcal{Q}^\dagger_{\nu'}\rangle\rangle = N_\mu(\delta_{\mu\mu'}\langle\langle \mathcal{Q}_\nu; \mathcal{Q}^\dagger_{\nu'}\rangle\rangle + \delta_{\mu\nu}\langle\langle \mathcal{Q}_{\mu'}; \mathcal{Q}^\dagger_{\nu'}\rangle\rangle). \tag{2.13}$$

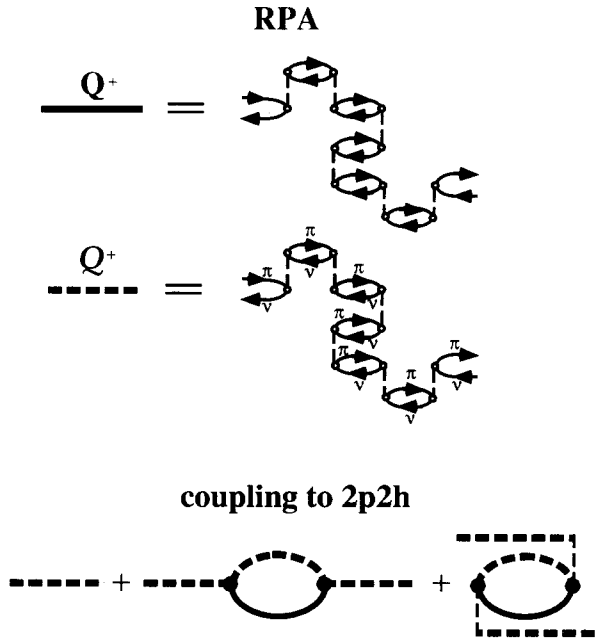

Fig. 1. Graphs summarized in the present approach. A vertical dashed line terminated by two open circles denotes the two-body interaction renormalized by the ground-state correlations beyond RPA.

As N_μ vanishes at zero temperature, this decoupling means that, in the study of GTR built on top of the ground state, we neglect all mixing to configurations higher than two-phonon ones. On the other hand it secures coupling to all possible $2p2h$ configurations.

The closed set of equations then undergoes the standard Fourier transformation to come to a complete set of equations for the Fourier images of the Green functions in Eqs. (2.10)–(2.12) and their backward process in the energy space η. Eliminating functions $\mathcal{G}^{--,+}(\eta)$ and $\mathcal{G}^{++,+}(\eta)$ by expressing them in terms of the functions $\mathcal{G}^{-,+}(\eta)$ and $\mathcal{G}^{+,+}(\eta)$, we finally obtain the set of the equations for the one-phonon propagators alone. This final set of equations for the propagation of p_π–h_ν phonon with energy η can be presented in a matrix form as

$$\begin{pmatrix} \mathcal{A} & \mathcal{B} \\ -\mathcal{B}' & -\mathcal{A}' \end{pmatrix} = \eta \begin{pmatrix} \mathcal{G}^{-,+}(\eta) \\ \mathcal{G}^{+,+}(\eta) \end{pmatrix}. \tag{2.14}$$

This looks formally like the SRPA equation [12] except that matrices $\mathcal{A}$, $\mathcal{B}$, $\mathcal{A}'$ and $\mathcal{B}'$ contain now the self-energy parts, which are functions of two-body matrix elements, the X and Y amplitudes, the ph and charge-exchange phonon energies ω_γ and $\overline{\omega}_\beta$, positive poles $\overline{\omega}_\beta + \omega_\gamma$ (two-phonon forward processes), negative poles $-(\overline{\omega}_\beta + \omega_\gamma)$ (two-phonon backward processes), and also the factor $(1 + \overline{N}_\beta + N_\gamma)$ coming from the decoupling in Eq. (2.13). The matrix elements of $\mathcal{A}$, $\mathcal{A}'$, $\mathcal{B}$, and $\mathcal{B}'$ are summarized in Appendix A.

The excitation energy η in the parent nucleus is defined as the solution of a determinant equation, whose matrix form is

$$\det||\boldsymbol{\Pi}(\eta)|| \equiv \det||(\mathcal{A}-\eta\hat{\delta}) - \mathcal{B}(\mathcal{A}'+\eta\hat{\delta})^{-1}\mathcal{B}'|| = 0. \tag{2.15}$$

The response is calculated by inverting the matrix $\boldsymbol{\Pi}(\eta)$. The strength function is proportional to the imaginary part of the response at complex energy with the factor $-1/\pi$. A technique has been developed in Ref. [15] for calculating the strength function, using the matrix inversion by Cramer's rule without finding the solutions of Eq. (2.15). This yields the strength function in the form

$$S(\eta) = \frac{1}{\pi}\mathrm{Im}\left\{\sum_{ii'}\frac{(-1)^{i+i'}\mathcal{M}_{ii'}(\eta+i\Delta)\Phi_i\Phi_{i'}}{\det||\boldsymbol{\Pi}(\eta+i\Delta)||}\right\}, \tag{2.16}$$

where $\mathcal{M}_{ii'}$ is the minor of the determinant $\det||\boldsymbol{\Pi}(\eta+i\Delta)||$ and Φ_i is the matrix element of the GT transition from the ground state to the one generated by charge-exchange phonons. The finite Δ plays the role of a smearing parameter in calculating the strength function. It can also account for coupling of $2p2h$ states to even more complicated configurations. In realistic calculations, to avoid spurious results, Δ is usually chosen to be sufficiently small such as the lowest moments of the strength function are insensitive to its actual value [12]. The overall procedure in the present formalism makes it physically equivalent to the extended RPA (ERPA) developed by Takayanagi et al. in Ref. [25], which is a generalization of the projected SRPA in Ref. [12]. In both our approach and ERPA the two-phonon (or $2p2h$) configurations are projected onto the one-phonon ($1p1h$) space including second-order correlation effects such as two-phonon backward processes. The calculations in both approaches can be carried out by coupling to many two-phonon ($2p2h$) configurations including those in the region of high-excitation energy. The ERPA was applied so far only to the calculations of M1 transitions [26] and the Coulomb sum rule in ^{40}Ca [27]. On the other hand, the two-step procedure in our approach, which uses the ph and charge-exchange phonons of the renormalized RPA to form the $2p2h$ configurations, makes the numerical calculations more feasible for heavy nuclei.

The kth moment, the energy centroid $\overline{E}$, the EWSR and the spreading width $\Gamma^{\downarrow}$ of the resonance distribution are calculated from the strength function $S(\eta)$ as

(a) the kth moment

$$m_k = \int_{E_1}^{E_2} S(\eta)\eta^k\, d\eta, \tag{2.17}$$

(b) the energy centroid $\overline{E}$ and the EWSR:

$$\overline{E} = \frac{m_1}{m_0}, \qquad \mathrm{EWSR} = m_1, \tag{2.18}$$

(c) the spreading width $\Gamma^{\downarrow}$:

$$\Gamma^{\downarrow} = \sqrt{\frac{m_2}{m_0} - (\overline{E})^2}. \tag{2.19}$$

Table 1
Average quantities extracted from the strength distribution of GTR in ^{90}Nb. The amounts of strength summed up in three energy intervals (i) below ($< E_<$), (ii) between ($E_<, E_>$) and (iii) above ($> E_>$) the GTR location are denoted as $S_<$, S_{GTR}, and $S_>$, respectively. The percentage of strength with respect to the Ikeda sum rule is given in parentheses. The centroid energy $\overline{E}$ and spreading width $\Gamma^{\downarrow}$ are calculated in the interval ($E_<, E_>$) with $E_<$ = 12 MeV, $E_>$ = 22 MeV. (A): results including two-phonon backward processes; (B): results neglecting these backward processes

		$\overline{E}$ (MeV)	$\Gamma^{\downarrow}$ (MeV)	$S_<$	S_{GTR}	$S_>$
a) Δ = 1 MeV	A	16.81	2.41	2.75 (9.17%)	19.06 (63.53%)	9.00 (30%)
	B	16.81	2.41	2.68 (8.93%)	19.08 (63.60%)	8.997 (29.99%)
b) Δ = 2 MeV	A	16.86	2.52	3.63 (12.1%)	16.45 (54.83%)	10.01 (33.37%)
	B	16.86	2.52	3.58 (11.93%)	16.47 (54.9%)	9.99 (33.30%)

3. Results

We have calculated the β_--strength distribution in ^{90}Nb and ^{208}Bi by coupling $p_\pi - h_\nu$ phonon excitations to natural parity $E\lambda^\pi$ (for ^{208}Bi) and unnatural parity $M\lambda^\pi$ phonon excitations (for ^{90}Nb) with $\lambda = 1 \sim 5$. All the one-phonon states with energy below 40 MeV and two-phonon states with energy up to 60 MeV are included. The calculations in ^{208}Bi use the single-particle energies defined in the standard oscillator potential. The levels around the Fermi surface are replaced, however, with the empirical values. For the calculations in ^{90}Nb the information about the empirical single particle levels is not complete, so the single-particle spectrum defined from a Woods–Saxon potential [28] is used around the Fermi surface. We adopt the M3Y nucleon–nucleon force as effective interaction, whose parameters are given in Refs. [11,26]. The matrix elements of M3Y interaction and RPA were calculated using some subroutines from the program code of Ref. [26].

The effects of ground-state correlations beyond RPA are found to be negligible in both nuclei (the factor D_{ph} is very close to 1). The calculated GTR strength functions for ^{90}Nb and ^{208}Bi are shown in Figs. 2 and 3, respectively. The results were obtained with Δ = 1 MeV, but our check has shown that the value of lowest moments of the strength function is rather stable against varying Δ from 0.1 MeV up to 2 MeV (see Table 1). The calculated strength function in ^{90}Nb agrees better with the experimental one up to 40 MeV (Fig. 2a) as compared to the results in Ref. [12] (dotted curve). At higher excitation energy the calculated results underpredict the experimental tail [18]. Despite the overall reasonable agreement with the data in Fig. 2a, some discrepancy still remains between the theoretical curve and the experimental histogram. This is not surprising as our formalism includes only the coupling to $2p2h$ configurations. Recent works on the GTR in medium mass nuclei (e.g. ^{54}Fe and ^{56}Fe) have shown that a full pf shell calculation is important in order to reproduce the quenching factor of the Gamow–Teller strength [29]. The calculations with the quasiparticle RPA including $2p2h$ configuration mixing in the ground state by Auerbach et al. [30] also concluded that higher-order correlations may significantly enlarge the quenching factor. In the present calculations it

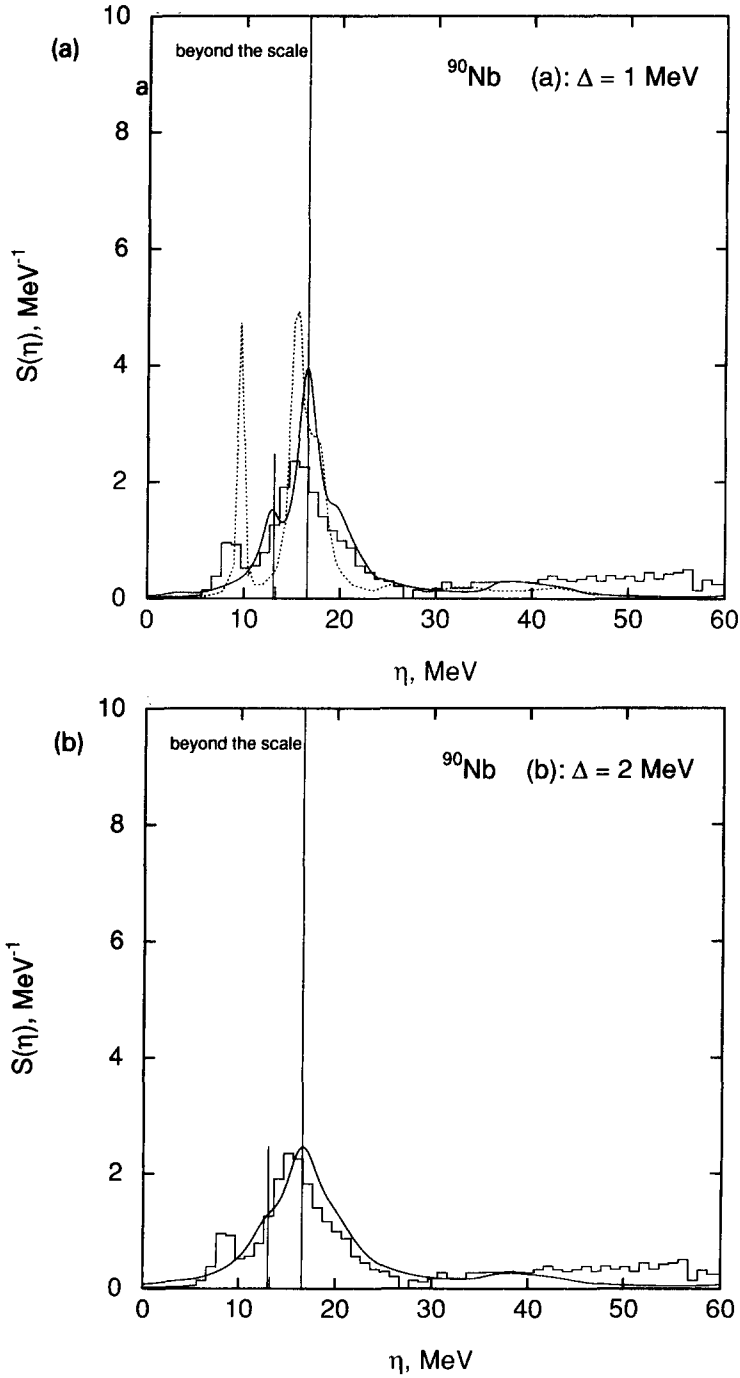

Fig. 2. Strength function of GTR in ^{90}Nb. Energies are measured with respect to the ground state of ^{90}Zr. The experimental strength distribution from Ref. [18] is shown by the histogram. Impulses show the RPA results. Dotted curves refer to the results of Ref. [12] while solid curves represent our results. Results obtained with Δ = 1 MeV are shown in (a), while (b) corresponds to those obtained with Δ = 2 MeV.

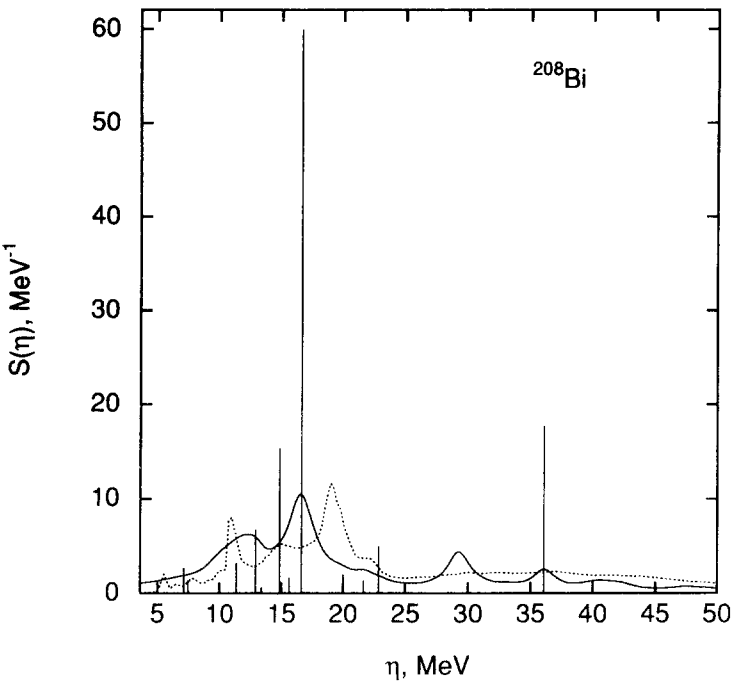

Fig. 3. Strength function of GTR in ^{208}Bi. Energies are measured with respect to the ground state of ^{208}Pb. Impulses show the RPA results. The dotted curve refers to the results of Ref. [12] while solid curves represent our results (Δ = 1 MeV).

is worth noticing that the experimental strength function in Ref. [18] can be reproduced quite well by doubling the smearing parameter Δ to 2 MeV. This may serve as a good evidence on the importance of mixing with configurations more complicated than $2p2h$ in ^{90}Nb (Fig. 2b). We also coupled the charge-exchange phonons, which generate the Gamow–Teller transitions in ^{90}Nb within the renormalized RPA, to the *ph* phonon states of natural parity. The change is found to be negligible as compared to the case with coupling to *ph* phonon states of unnatural parity. Concerning the experimental strength function for the GTR in ^{208}Bi, it is not available at present. Wakasa et al. [18] have performed the extensive measurement of the differential cross sections at angles $\theta_{\rm lab}$ between 0° and 15° with about 1.2° steps and of the polarization transfer D_{NN} at angles $\theta_{\rm lab}$ = 0°, 4°, 7°, and 10° for the ^{208}Pb($\boldsymbol{p},\boldsymbol{n}$) reaction at T_p = 295 MeV. They found that the polarization transfer D_{NN} is very sensitive to the multipolarities J^π. This made the multipole analysis much more complicate as one has to perform it not only with differential cross sections but also with polarization transfer observables at finite angles.

The main peak of the GTR strength function in ^{209}Bi (Fig. 3) is located at 16.6 MeV compared to the experimental value 19.2 MeV [17]. The oscillator levels far above the Fermi surface is obviously the reason for this deviation. As a matter of fact an energy of GTR closer to the experimental value was achieved by reducing the standard oscillator strength by 4∼5%. By doing so, we also improves the similarity between our results

Table 2
Average quantities extracted from the strength distribution of GTR in ^{208}Bi. Notation is the same as in Table 1 with $E_< = 8$ MeV, $E_> = 25$ MeV

	$\overline{E}$ (MeV)	$\Gamma^{\downarrow}$ (MeV)	$S_<$	S_{GTR}	$S_>$
A	15.43	3.87	9.62 (7.3%)	75.32 (57.1%)	50.26 (38.1%)
B	15.28	3.85	10.73 (8.1%)	63.97 (48.5%)	62.14 (47.1%)

and the ones of Refs. [12,13]. However, we would like to keep the standard parameters of the potential and effective interaction unchanged throughout all calculations. The coupling to $2p2h$ states spreads the GTR up to around 60 MeV. The sum rule has been examined in three energy intervals: i) below the GTR location, ii) in the GTR location and iii) above it. The results are summarized in Tables 1 and 2, where the calculated values of the spreading width $\Gamma^{\downarrow}$ and the energy centroid $\overline{E}$ of the GTR in the resonance location are also shown. In the GTR region in ^{208}Bi (Table 2) the integrated strength amounts to 57% of the Ikeda sum rule compared to $60\pm15\%$ found in experiments [17]. The tail in the energy region above the GTR amounts to 38% of the Ikeda sum rule, while there is 7.3% of the sum rule distributed in the lower-energy region (i). The spreading width $\Gamma^{\downarrow}$ is 3.87 MeV compared to the experimental value 3.72 MeV. For ^{90}Nb (Table 1) we found around 30% of the Ikeda sum rule in the region of excitation energies higher than 22 MeV compared to around 40% extracted for the first time in experiments [18]. We argue that the nature of the continuum in this energy region still remains an open question, requiring further measurements. The spreading width and the energy centroid of the GTR in ^{90}Nb are $\Gamma^{\downarrow} \simeq 2.4$ MeV and $\overline{E} \simeq 16.8$ MeV, respectively. The experimental values for these quantities are not available upon the writing of the present paper. The calculated total β_- strength of GTR up to more than 60 MeV amounts to around 103% of the Ikeda sum rule in both nuclei. This is in agreement with the empirical observation on the contribution of the β_+ transitions of around $1.7\pm0.2\%$ of the GTR sum rule. Inclusion of two-phonon backward processes made the GTR more collective in the resonance region. These effects are better seen in ^{208}Bi (see Table 2). Further study with different choices of the residual interaction is highly desirable to see whether these effects interfere constructively or destructively with the damping of GTR. A test by switching off the tensor part of the M3Y interaction confirms that the tensor part is responsible for pushing the GTR distribution up to higher energy with a long high-lying tail [8,12]. Our calculations and those in Refs. [11,12] show that the use of a non-separable interaction including the tensor force in calculating the $1p1h$–$2p2h$ configuration mixing is decisive in achieving an adequate GTR strength distribution up to excitation energies of 60 MeV. For a comparison, we refer to Refs. [14,16] (Fig. 4). The authors of Ref. [14] adopted a separable force whose parameters were adjusted from nucleus to nucleus to reproduce the lowest and resonance energies found in experiments. The GTR strength below 30 MeV in their calculations already exhausts the Ikeda sum rule (dotted curves in Fig. 4). The GTR in ^{208}Bi calculated in Ref. [16] is concentrated in a narrow region around (18∼24 MeV). The energy of the main peak of the GTR is

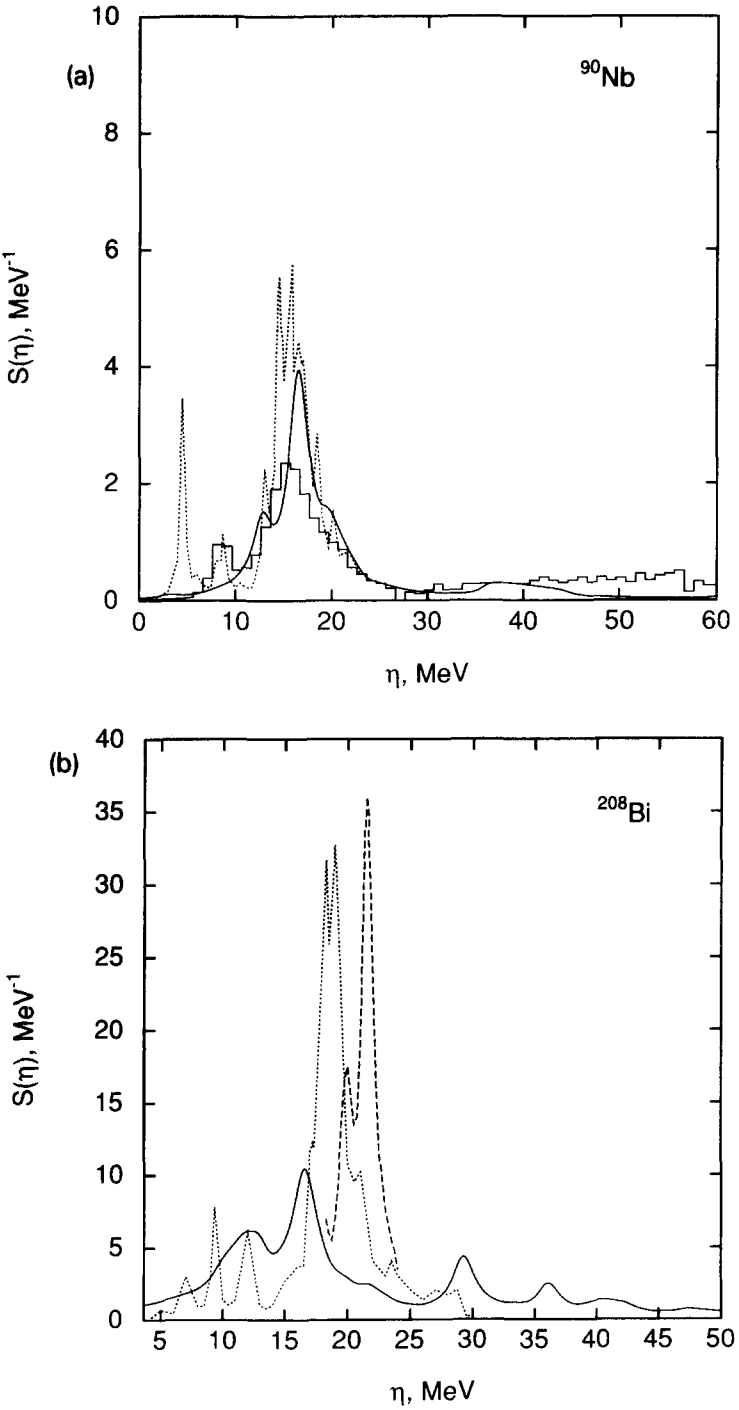

Fig. 4. Strength function of GTR in ^{90}Nb (a) and ^{208}Bi (b) (solid curve) in comparison with Refs. [14] (dotted curve) and [16] (dashed curve).

Table 3
Average quantities extracted from the strength distribution of GTR in ^{208}Bi at several temperature. Notation is the same as in Tables 1 and 2

T (MeV)	$\overline{E}$ (MeV)	$\Gamma^{\downarrow}$ (MeV)	$S_<$	$S_{\rm GTR}$	$S_>$
0	15.43	3.87	9.62 (7.3%)	75.32 (57.1%)	50.26 (38.1%)
2	15.33	3.91	9.71 (7.4%)	75.78 (57.4%)	45.13 (34.2%)
4	15.37	3.93	9.33 (7.1%)	79.36 (60.1%)	49.24 (37.3%)
6	15.15	3.91	11.34 (8.6%)	87.47 (66.3%)	45.25 (32.0%)

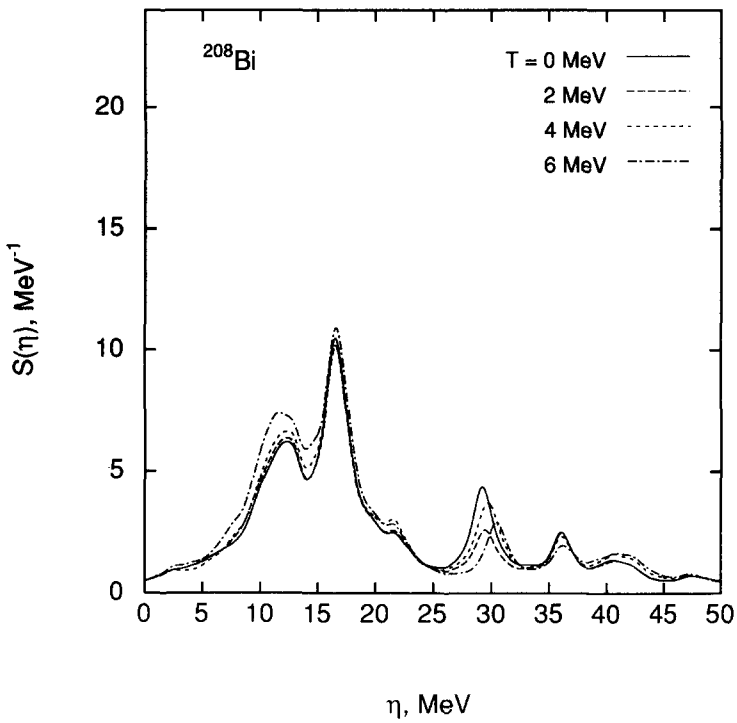

Fig. 5. Strength function of GTR in ^{208}Bi at several temperatures. Notation of curves is given in the figure.

higher than the experimental value by 2~4 MeV depending on the type of the Skyrme interaction in use. (The dashed curve in Fig. 4b corresponds to the results obtained in Ref. [16] using the SIII force.) There is no indication in Ref. [16] on how the rest of the sum rule is distributed beyond the GTR. Both approaches in Refs. [14,16] give a GTR spreading width in ^{208}Bi, which is narrower than the experimental findings by around 20%.

We also performed the calculations of the GTR strength function at several temperatures up to T = 6 MeV. The results of calculations in ^{208}Bi are displayed in Fig. 5. The values of the integrated strength, the centroid energy and the spreading width are summarized in Table 3. The strength in the GTR region in ^{208}Bi increases less than 10% at T = 6 MeV while it decreases accordingly in the higher-energy tail. The spreading

width $\Gamma^{\downarrow}$ is broadened by less than 2%. The centroid energy in the interval ii) moves downward by less than 300 keV (at $T = 6$ MeV). Our calculations also show that the temperature dependence of the strength function of GTR in ^{90}Nb is negligible.

4. Conclusions

We have proposed a microscopic approach for the calculations of $1p1h$–$2p2h$ configuration mixing in the GTR. There are no free parameters in the present approach. The advantages of the present approaches as compared to other models developed so far [11–13,15,16] can be summarized as follows. The present approach is a non-perturbative one, where the ground-state correlations beyond RPA and the two-phonon backward processes are properly taken into account. Adopting the M3Y interaction, this approach includes the coupling to low- as well as high-lying two-phonon configurations up to 60 MeV. The combination of empirical single-particle levels or the levels from a Woods–Saxon potential with those from a standard harmonic oscillator potential allows us to simulate effectively the influence of the region of high excitation energy in the continuum. Last but not least, the two-time Green function method used in our formalism makes its extension to non-zero temperature natural.

The results of our calculations for ^{90}Nb and ^{208}Bi show that the present formalism can provide a good account for recent experimental findings on the spreading properties of these nuclei. Our results reconfirm that one may not need recoursing to Δ isobar–hole admixtures for an explanation of the GTR quenching. This statement is also supported by the recent empirical observation [18]. Our results show that the effect of ground-state correlations beyond RPA is negligible for the GTR, while the two-phonon backward processes do influence, although slightly, its collectivity. Therefore it is quantitatively safe to put $D_{ph} = 1$ in further numerical calculations of GTR avoiding the procedure of solving self-consistently a set of non-linear equations. We also found that the GTR is rather stable against temperature up to $T = 6$ MeV.

In order to explore further the predictability of our approach it would be interesting to extend the present formalism to the study of unstable doubly closed-shell and neutron-rich nuclei such as ^{132}Sn. The decay measurements of these nuclei, including the decay into the isobaric analog and Gamow–Teller states, are now becoming possible with the RI Beam Factory project at the RIKEN Accelarator Facility [31]. This may serve as a subject in our forthcoming study.

Acknowledgements

Numerical calculations were carried out by a 64-bit Alpha AXP work-station running Digital UNIX (OSF/1) at the Computer Center of RIKEN. The authors are grateful to K. Takayanagi for providing the program code of matrix elements of the M3Y interaction and RPA and N. Onishi for valuable discussions and comments. Thanks are also due to T. Wakasa and H. Sakai for discussions and for providing the experimental data of Ref. [18] before publication.

Appendix A. Matrix elements in calculations of strength function

In this appendix we give the explicit form of the matrix elements of $\mathcal{A}$, $\mathcal{A}'$, $\mathcal{B}$ and $\mathcal{B}'$ in Eqs. (2.14) and (2.15). They are

$$\mathcal{A}_{\alpha\zeta} = \overline{\omega}_\alpha \delta_{\alpha\zeta} + \sum_{\beta\gamma} (1 + \overline{N}_\beta + N_\gamma) \times \left\{ \frac{V^\gamma_\beta(\alpha) V^\gamma_\beta(\zeta)}{\eta - \overline{\omega}_\beta - \omega_\gamma} - \frac{[V^\gamma_\beta + V^\gamma_\alpha(\beta)][V^\gamma_\beta(\zeta) + V^\gamma_\zeta(\beta)]}{\eta + \overline{\omega}_\beta + \omega_\gamma} \right\}, \tag{A.1}$$

$$\mathcal{B}_{\alpha\zeta} = \sum_{\beta\gamma} (1 + \overline{N}_\beta + N_\gamma) \times \left\{ \frac{V^\gamma_\beta(\alpha)[V^\gamma_\beta(\zeta) + V^\gamma_\zeta(\beta)]}{\eta - \overline{\omega}_\beta - \omega_\gamma} - \frac{[V^\gamma_\beta + V^\gamma_\alpha(\beta)] V^\gamma_\beta(\zeta)}{\eta + \overline{\omega}_\beta + \omega_\gamma} \right\}, \tag{A.2}$$

$$\mathcal{A}'_{\alpha\zeta} = \overline{\omega}_\alpha \delta_{\alpha\zeta} + \sum_{\beta\gamma} (1 + \overline{N}_\beta + N_\gamma) \times \left\{ \frac{[V^\gamma_\beta + V^\gamma_\alpha(\beta)][V^\gamma_\beta(\zeta) + V^\gamma_\zeta(\beta)]}{\eta - \overline{\omega}_\beta - \omega_\gamma} - \frac{V^\gamma_\beta(\alpha) V^\gamma_\beta(\zeta)}{\eta + \overline{\omega}_\beta + \omega_\gamma} \right\}, \tag{A.3}$$

$$\mathcal{B}'_{\alpha\zeta} = \sum_{\beta\gamma} (1 + \overline{N}_\beta + N_\gamma) \times \left\{ \frac{[V^\gamma_\beta + V^\gamma_\alpha(\beta)] V^\gamma_\beta(\zeta)}{\eta - \overline{\omega}_\beta - \omega_\gamma} - \frac{V^\gamma_\beta(\alpha)[V^\gamma_\beta(\zeta) + V^\gamma_\zeta(\beta)]}{\eta + \overline{\omega}_\beta + \omega_\gamma} \right\}. \tag{A.4}$$

A Greek index denotes a pair of phonon number i and its angular momentum J with parity π, e.g. $\alpha \equiv J^\pi i$. The quantity $\overline{N}$ stands for the occupation number of charge-exchange phonon with energy $\overline{\omega}$. The vertex function $V^\gamma_\beta(\alpha)$ contains the matrix elements of the two-body interaction. Its general form is

$$V^\gamma_\beta(\alpha) = \langle 0 | \mathcal{Q}_\beta H_V [Q^\dagger_\gamma \otimes \mathcal{Q}^\dagger_\alpha]_\beta | 0 \rangle, \tag{A.5}$$

where $[Q^\dagger_\gamma \otimes \mathcal{Q}^\dagger_\alpha]_\beta$ denotes the tensor product. The expression of $V^\gamma_\beta(\alpha)$ in terms of the amplitudes X and Y for the β_--transitions of GTR is identical to the one in the QPM up to the reduced matrix elements of the two-body interaction including angular-momentum coupling in the case of spherical nuclei. Therefore we refer the reader to the monograph in Ref. [15] and references therein for further details.

Matrices $\mathcal{A}'$, $\mathcal{B}$ and $\mathcal{B}'$ in Eq. (2.14) arise due to the backward processes described by the Green functions $\mathcal{G}^{+,+}$ and $\mathcal{G}^{++,+}$. If the backward processes are neglected one recovers from Eq. (2.15) at $T = 0$ the determinant equation in the QPM [14]:

$$\det \left\| (\eta - \overline{\omega}_\alpha)\delta_{\alpha\zeta} - \sum_{\beta\gamma} \frac{V^\gamma_\beta(\alpha) V^\gamma_\beta(\zeta)}{\eta - \overline{\omega}_\beta - \omega_\gamma} \right\| = 0. \tag{A.6}$$

References

[1] K. Ikeda, S. Fujii and J.I. Fujita, Phys. Rev. Lett. 3 (1963) 271.
[2] R.R. Doering, A. Galonsky, D.M. Patterson and G.F. Bertsch, Phys. Rev. Lett. 35 (1975) 1961.
[3] D.H. Wilkinson, Phys. Rev. C 7 (1973) 930; Nucl. Phys. A 209 (1973) 470; A 225 (1974) 365.
[4] K. Sugimoto, A. Mizobuchi, T. Minamizono and Y. Nojiri, J. Phys. Soc. Jpn. Suppl. 34 (1973) 158; T. Minamizono, J.W. Hugg, D.G. Mavis, T.K. Saylor, H.F. Glavish and S.S. Hanna, Phys. Lett. B 61 (1976) 155.
[5] K. Shimizu, M. Ichimura and A. Arima, Nucl. Phys. A 226 (1974) 282.
[6] M. Ericson, A. Figureau and C. Thevenet, Phys. Lett. B 45 (1973) 19; M. Rho, Nucl. Phys. A 231 (1974) 493; E. Oset and M. Rho, Phys. Rev. Lett. 42 (1979) 47.
[7] L.S. Towner and F.C. Khanna, Phys. Rev. Lett. 42 (1979) 51.
[8] A. Arima and H. Hyuga, *in* Meson in nuclei, ed. D. Wilkinson (North-Holland, Amsterdam 1979) p. 683.
[9] F. Osterfeld, Rev. Mod. Phys. 64 (1992) 491.
[10] C. Gaarde, J. Rapaport, T.N. Taddeucci, C.D. Goodman, C.J. Horen and E. Sugarbaker, Nucl. Phys. A 369 (1981) 258.
[11] G.F. Bertsch and I. Hamamoto, Phys. Rev. C 26 (1982) 1323.
[12] S. Drożdż, V. Klempt, J. Speth and J. Wambach, Phys. Lett. B 166 (1986) 18; S. Drożdż, S. Nishizaki, J. Speth and J. Wambach, Phys. Rep. 197 (1990) 1.
[13] T. Udagawa, D.P. Knobles. and S.A. Stotts, Nucl. Phys. A 577 (1994) 67c.
[14] V.A. Kuzmin and V.G. Soloviev, J. Phys. G 10 (1984) 1507.
[15] V.G. Soloviev, Theory of Atomic Nuclei – Quasiparticles and Phonons (IOP, Bristol, 1992).
[16] G. Colò, N. Van Giai, P.F. Bortignon and R.A. Broglia, Phys. Rev. C 50 (1994) 1496.
[17] H. Akimune, I. Daito, Y. Fujita, M. Fujiwara, M.B. Greenfield, M.N. Harakeh, T. Inomata, J. Jänecke, K. Katori, S. Nakayama, H. Sakai, Y. Sakemi, M. Tanaka and M. Yosoi, Phys. Rev. C 52 (1995) 604.
[18] T. Wakasa, H. Sakai, H. Okamura, H. Otsu, S. Fujita, Y. Satou, T. Uesaka. M.B. Greenfield, S. Ishida, N. Sakamoto and K. Hatanaka, Gamow-Teller strength in ^{90}Nb studied via multipole decomposition analysis of the ^{90}Zr(p,n) reaction at 295 MeV, Int. Symp. on Non-Nucleonic Degrees of Freedom detected in Nucleus (Sept. 2–5, 1996, Osaka, Japan) (to be published).
[19] K. Hara, Prog. Theor. Phys. 32 (1964) 88; K. Ikeda, T. Udagawa and H. Yamaura, Prog. Theor. Phys. 33 (1965) 22.
[20] M. Hage-Hassan and M. Lambert, Nucl. Phys. A 188 (1972) 545.
[21] F. Catara, N. Dinh Dang and M. Sambataro, Nucl. Phys. A 579 (1994) 1.
[22] N.N. Bogolyubov and S.V. Tyablikov, Sov. Phys. Dokl. 4 (1959) 589; R. Kubo, M. Toda and N. Hashitsume, Statistical Physics II (Springer, Berlin, 1985) p. 201.
[23] D.N. Zubarev, Sov. Phys. Usp. 3 (1960) 320.
[24] N. Dinh Dang and N. Zuy Thang, J. Phys. G 14 (1988) 1471; G 16 (1990) 231; N. Dinh Dang, Nucl. Phys. A 504 (1989) 143; J. Phys. G 16 (1990) 623; Phys. Rep. 264 (1996) 123.
[25] K. Takayanagy, K. Shimizu and A. Arima, Nucl. Phys. A 447 (1988) 205.
[26] K. Takayanagi, K. Shimizu and A. Arima, Nucl. Phys. A 481 (1988) 313.
[27] K. Takayanagi, Nucl. Phys. A 522 (1991) 523.
[28] V.A. Chepurnov, Sov. J. Nucl. Phys. 6 (1967) 955; K. Takeuchi and P.A. Moldauer, Phs. Lett. B 28 (1969) 384.
[29] E. Caurier, G. Martínez-Pinedo, A. Poves and A.P. Zuker, Phys. Rev. C 52 (1995) R1736; K. Langanke, D.J. Dean, P.B. Radha, Y. Alhassid and S.E. Koonin, Phys. Rev. C 52 (1995) 718.
[30] N. Auerbach, G.F. Bertsch, B.A. Brown and L. Zhao, Nucl. Phys. A 556 (1993) 190.
[31] RARF Collaboration, Basic Science in RI Beam Factory (RIKEN Accelerator Research Facility, August 1994) p. 135.